ФИЗИКА ЭЛЕМЕНТАРНЫХ ЧАСТИЦ И АТОМНОГО ЯДРА
2014. Т. 45. ВЫП. 4

NNLL THRESHOLD RESUMMATION FOR TOP-PAIR AND SINGLE-TOP PRODUCTION

N. Kidonakis

Kennesaw State University, Physics #1202, Kennesaw, GA, USA

ФИЗИКА ЭЛЕМЕНТАРНЫХ ЧАСТИЦ И АТОМНОГО ЯДРА
2014. Т. 45. ВЫП. 4

NNLL THRESHOLD RESUMMATION FOR TOP-PAIR AND SINGLE-TOP PRODUCTION

N. Kidonakis

Kennesaw State University, Physics #1202, Kennesaw, GA, USA

I discuss threshold resummation at NNLL accuracy in the standard moment-space approach in perturbative QCD for top-pair and single-top production. For top-quark pair production, I present new approximate NNLO results for the total cross section and for the top-quark transverse momentum and rapidity distributions at 8 TeV LHC energy. I discuss the accuracy of the soft-gluon approximation and show that the NLO and NNLO approximate results from resummation are practically indistinguishable from exact NLO and partial NNLO results. For single-top production I present new approximate NNLO results for the total cross sections in all three channels at the LHC and also for the top-quark transverse momentum distributions in t-channel production and in top-quark associated production with a W boson. For both $t\bar{t}$ and single-top production, the agreement of theoretical results with LHC and Tevatron data is excellent.

Рассматривается NNLL пересуммирование на пороге в рамках стандартного импульсного приближения пертурбативной КХД для рождения пары и одиночного топ-кварка. Рождение пары топ-кварков описывается приближенными NNLO результатами для полного сечения в зависимости от поперечного импульса топ-кварка и распределения по быстроте при энергии 8 ГэВ на LHC. Обсуждается точность приближения мягкого глюона; показано, что приближенные NLO и NNLO результаты, полученные после пересуммирования, практически неотличимы от точного NLO и частного случая NNLO. Для случая рождения одного топ-кварка в рамках нового приближенного NNLO описания получены полные сечения во всех трех каналах, а также для распределений по поперечному импульсу топ-кварка в t-канале и при рождении топ-кварка, связанного с W-бозоном. Получено отличное согласие с экспериментальными данными LHC и тэватрона как для рождения пары $t\bar{t}$, так и для рождения одиночного t-кварка.

PACS: 12.38.Bx; 12.38.Cy; 14.65.Ha

INTRODUCTION

Threshold resummation is important for increasing the theoretical accuracy of top-quark total and differential cross sections at hadron colliders. The top-quark is the heaviest known elementary particle and its study is of unique importance both theoretically and in experiments at the LHC and previously at the Tevatron. The top-quark cross section is well known to receive large contributions from soft-gluon emission near partonic threshold. Resummation of soft-gluon corrections at the next-to-leading-logarithm (NLL) accuracy [1,2] and beyond depends on the color structure of the hard scattering.

Soft-gluon resummation was developed recently at the next-to-next-to-leading-logarithm (NNLL) accuracy in various approaches for $t\bar{t}$ differential [3–6] and

total [3–5, 7, 8] cross sections. It is very important to note that although all these approaches are formally NNLL, they are quite different from each other both theoretically and numerically, and «NNLL» can mean different things since the variables used for the threshold logarithms, the formalism employed, and the practical choices made in its implementation vary widely. Differences between the approaches include performing the resummation for the double-differential cross section in single-particle-inclusive (1PI) [4–6] and/or pair-invariant-mass (PIM) [3] kinematics versus doing the resummation solely for the total cross section using production threshold [7, 8]; using moment-space resummation in perturbative QCD [4,6,7] versus using Soft-Collinear Effective Theory (SCET) [3,5,8]; choices for the analytical and numerical implementation of the expressions and for damping factors away from threshold; and keeping subleading terms of various origins. A review explaining in detail many of the differences can be found in [9]. In the double-differential approach, the resummation is sensitive to the kinematical invariants of the partonic process; this sensitivity is lost in the total-cross-section-only approach where the production threshold (also known as absolute threshold) that is used is simply a special case of the more general partonic threshold employed in 1PI and PIM differential kinematics (see discussion in [9]). We note that the formalism presented here is the only calculation using the moment-space perturbative-QCD NNLL resummation for the double-differential cross section in 1PI kinematics, $d\sigma/dp_T dY$, to calculate approximate NNLO total cross sections and transverse momentum, p_T, and rapidity, Y, distributions for both top-pair production [4, 6] and single-top production [10–12].

In the next section, we briefly describe our resummation formalism. In Sec. 2, we present results for top-pair production, including the total cross section, the top-quark transverse momentum distribution, and the top-quark rapidity distribution. New results for 8 TeV LHC energy are presented and compared with results at 7 TeV. A discussion of the excellent accuracy of the soft-gluon approximation at NLO and NNLO is also presented. In Sec. 3, we discuss new results for single-top production in the t, s, and tW channels. New results for the total cross sections at 8 TeV LHC energy are shown together with (updated) results at 7 TeV. Furthermore, new theoretical calculations and results for the top (and antitop) transverse momentum distributions in t-channel production are presented at LHC and Tevatron energies. A new calculation for the top-quark transverse momentum distribution in tW production at the LHC is also presented. We conclude in the last section.

1. RESUMMATION AT NNLL

We begin with a brief description of our formalism for NNLL resummation of soft-gluon corrections. We consider partonic processes of the form

$$f_1(p_1) + f_2(p_2) \to t(p) + X, \tag{1.1}$$

where f_1 and f_2 represent partons (quarks or gluons), t represents the top-quark, and X represents additional final-state particles. The partonic cross section explicitly involves the kinematical invariants $s = (p_1+p_2)^2$, $t_1 = (p_1-p)^2-m_t^2$, $u_1 = (p_2-p)^2-m_t^2$, with m_t being the top-quark mass, as well as factorization scale μ_F and the renormalization scale μ_R. The physical cross section is in principle independent of μ_F and μ_R, but a dependence appears when we truncate the infinite perturbative series at finite order.

Near partonic threshold for the production of the top-quark final state, the cross section receives logarithmic contributions that arise from incomplete cancellations between virtual terms and terms from soft-gluon emission. These contributions are of the form $[\ln^l(s_4/m_t^2)/s_4]_+$, where $s_4 = s+t_1+u_1$ measures the distance from partonic threshold. Soft-gluon resummation depends critically on the color structure of the partonic process as well as its kinematics.

The resummation of threshold logarithms is performed in the moment space, it is based on the factorization properties of the cross section, and it employs the eikonal approximation for describing the emission of soft gluons from partons in the hard scattering. By taking moments, logarithms of s_4 produce powers of $\ln N$, with N being the moment variable. The resummation was first performed at NLL accuracy in [1,2] and at NNLL accuracy in [4].

We factorize the moments of the partonic cross section in dimensional regularization as [1,2]

$$\hat{\sigma}_{f_1f_2\to tX}(N,\epsilon) = \psi_{f_1/f_1}(N,\mu_F,\epsilon)\,\psi_{f_2/f_2}(N,\mu_F,\epsilon)H_{IL}^{f_1f_2\to tX}(\alpha_s(\mu_R))\times$$
$$\times\; S_{LI}^{f_1f_2\to tX}\left(\frac{m_t}{N\mu_F},\alpha_s(\mu_R)\right)\prod_j J_j(N,\mu_F,\epsilon)+\mathcal{O}(1/N), \quad (1.2)$$

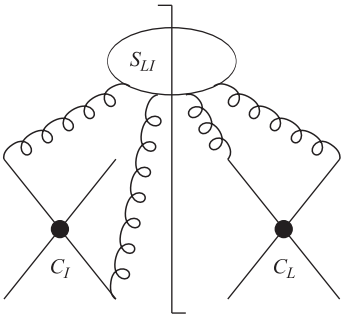

Fig. 1. The soft-gluon matrix S_{LI}. The eikonal lines connect with color tensors c_I and c_L

where ψ are center-of-mass distributions for the incoming partons; H_{IL} is the N-independent hard matrix in the space of color exchanges (with color indices I, L); S_{LI} is the soft matrix; and J are functions for massless partons in the final state. More details about the definitions of these functions and the construction of the eikonal cross section can be found in [2].

The hard-scattering matrix involves contributions from the amplitude of the process and the complex conjugate of the amplitude, $H_{IL} = h_L^*\,h_I$. The soft function S_{LI} represents the emission of noncollinear soft gluons from the partons in the scattering. The color tensors of the hard scattering connect together the eikonal lines to which soft gluons couple (see Fig. 1).

The N-dependence of the soft matrix S_{LI} can be resummed by renormalization group analysis. S_{LI} satisfies the renormalization group equation [1, 2]

$$\left(\mu\frac{\partial}{\partial\mu}+\beta(g_s)\frac{\partial}{\partial g_s}\right) S_{LI} = -(\Gamma_S^\dagger)_{LB}S_{BI} - S_{LA}(\Gamma_S)_{AI}, \tag{1.3}$$

where β is the QCD beta function and $g_s^2 = 4\pi\alpha_s$. Γ_S is the soft anomalous dimension matrix and it is calculated in the eikonal approximation by explicit renormalization of the soft function.

The exponentiation of logarithms of N in the functions ψ and J in the factorized cross section, together with the solution of the renormalization group equation (1.3), provide us with the complete expression for the resummed (double-differential) partonic cross section in the moment space

$$\begin{aligned}\hat{\sigma}_{\rm res}(N) = \exp\left[\sum_i E^{f_i}(N_i)\right]\exp\left[\sum_j E'^{f_j}(N')\right]\times \\ \times\exp\left[\sum_i 2\int_{\mu_F}^{\sqrt{s}}\frac{d\mu}{\mu}\,\gamma_{f_i/f_i}(\alpha_s(N_i,\mu))\right]\times \\ \times{\rm Tr}\left\{H^{f_1f_2\to tX}\left(\alpha_s(\sqrt{s})\right)\exp\left[\int_{\sqrt{s}}^{\sqrt{s}/\tilde{N}'}\frac{d\mu}{\mu}\,\Gamma_S^{\dagger\,f_1f_2\to tX}\left(\alpha_s(\mu)\right)\right]\times\right. \\ \left.\times S^{f_1f_2\to tX}\left(\alpha_s\left(\frac{\sqrt{s}}{\tilde{N}'}\right)\right)\exp\left[\int_{\sqrt{s}}^{\sqrt{s}/\tilde{N}'}\frac{d\mu}{\mu}\,\Gamma_S^{f_1f_2\to tX}\left(\alpha_s(\mu)\right)\right]\right\}.\end{aligned} \tag{1.4}$$

The first and second exponents in Eq. (1.4) control collinear and soft-gluon emission [13, 14] from incoming and outgoing partons, respectively, while the third exponent controls the factorization scale dependence of the cross section. Explicit expressions for these exponents can be found in [15]. The evolution of the soft-gluon function is controlled by the soft anomalous dimension matrix Γ_S via the solution to Eq. (1.3).

The ultraviolet poles in loop diagrams involving eikonal lines play a direct role in the renormalization group evolution equations that are used in the calculation of the soft anomalous dimensions [1, 2, 16]. The soft anomalous dimension matrices in our formalism have been calculated at two loops for the partonic processes in top-pair production in [4, 16] and for single-top production in [10–12].

2. TOP-PAIR PRODUCTION

The threshold resummation formalism discussed here has been used to calculate top-pair production at the Tevatron and the LHC [4, 6]. We expand the NNLL resummed cross section to NNLO. We add the NNLO soft-gluon corrections from this expansion to the exact NLO [17–19] expressions and denote the result as approximate NNLO. Here we present new results for the current 8 TeV LHC energy for the total cross section and the top-quark transverse momentum and rapidity distributions. The factorization and renormalization scales are set equal to each other and denoted by μ. Throughout we use the MSTW2008 [20] NNLO parton distribution functions (pdf).

We begin by examining the validity and numerical accuracy of the threshold soft-gluon approximation by comparing exact NLO and approximate NLO results (with $\mu = m_t$) for the total $t\bar{t}$ cross section and the top-quark p_T distribution. The comparison is shown in plots of Fig. 2, *a*. The top plot of Fig. 2, *a* displays the exact and approximate NLO corrections, i.e., $\mathcal{O}(\alpha_s)$ corrections, for the total top-pair cross section at 7 and 8 TeV LHC energy. We note that the approximation is excellent with only around 2 to 3% difference between approximate and exact corrections. The approximate results include only $q\bar{q}$ and gg channels (for which resummation is performed), while the exact results also include the qg and $\bar{q}g$ channels (the contribution from the latter two channels is quite small). In fact, if only the sum of the $q\bar{q}$ and gg channels are included in the exact result, the difference between approximate and exact corrections is only 1 to 2%. This very good agreement between exact and approximate NLO corrections also holds separately for the $q\bar{q}$ and gg channels. If one compares the total NLO cross section (i.e., the sum of the leading-order cross section plus the NLO corrections), the difference between approximate and exact results is entirely negligible, well below 1%. This excellent agreement between exact and approximate NLO results is true not only for the total cross section but also for differential distributions. The bottom plot of Fig. 2, *a* shows that the exact NLO transverse momentum distribution of the top quark is again almost identical to the approximate NLO result (the results are for 8 TeV LHC energy and $m_t = 173$ GeV). We note that there are some choices to be made in the analytical structure and numerical implementation of the calculation, all strictly equivalent at partonic threshold but not entirely equivalent away from it, and different choices can give somewhat different results. The agreement between exact and approximate results shown here proves the validity, accuracy, and importance of our approach and the appropriateness of our choices, and it is the motivation for studying higher-order soft-gluon corrections in the same approach and with the same choices. As we will discuss shortly, recent partial NNLO results are also in excellent agreement with the approximate NNLO results from our formalism, thus further proving the advantages and accuracy of our approach.

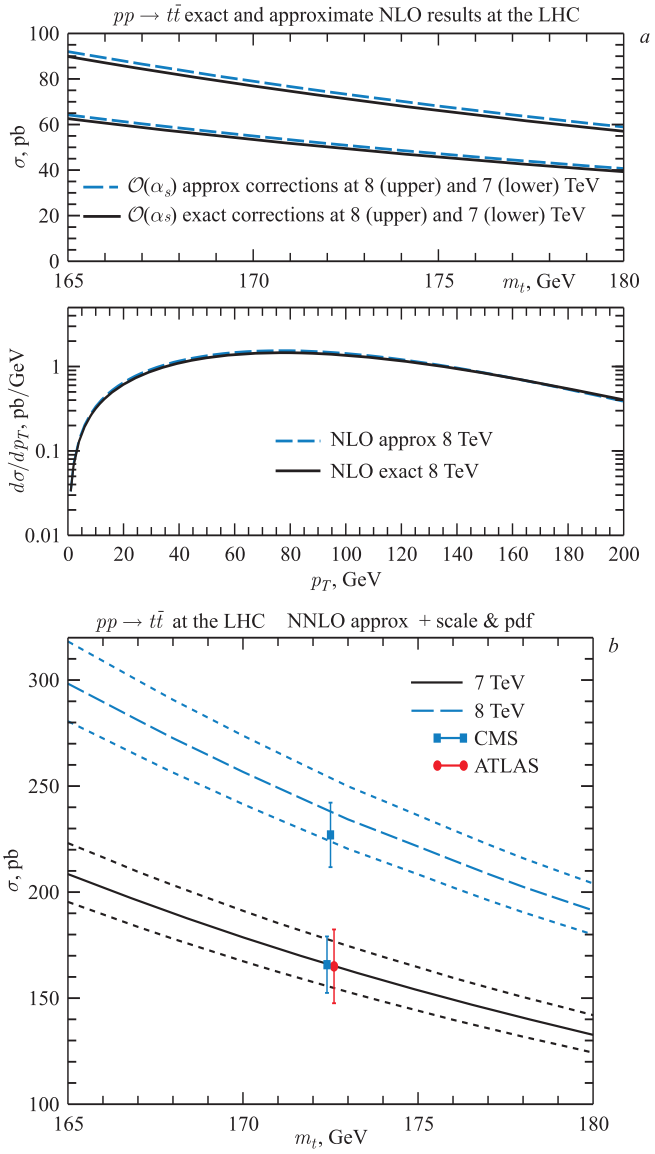

Fig. 2. *a*) Comparison of exact and approximate NLO results for the total top-pair cross section and top-quark p_T distribution; *b*) NNLO approximate top-pair total cross section compared with data at the LHC

In Fig. 2, *b*, we show the NNLO approximate total top-pair production cross section at the LHC at 8 TeV energy, and for comparison also at 7 TeV energy, as a function of top-quark mass. Here we have set $\mu = m_t$ for our central results. The uncertainties from scale variation and from the pdf are added in quadrature. The results at 7 TeV are compared with ATLAS and CMS data [21, 22]. The 8 TeV results are compared with recent CMS data [23]. Excellent agreement is found between theory and experiment for both the energies.

The new result for the current 8 TeV LHC energy with a top-quark mass $m_t = 173$ GeV and using MSTW2008 NNLO pdf is

$$\sigma_{t\bar{t}}^{\text{NNLO approx}}(m_t = 173 \text{ GeV},\ 8 \text{ TeV}) = (234^{+10}_{-7} \pm 12) \text{ pb}, \qquad (2.1)$$

where the first uncertainty is from scale variation $m_t/2 < \mu < 2m_t$ and the second is from the pdf at 90% C.L. We note that independent variation of μ_F and μ_R does not increase the scale uncertainty at LHC energies. At 7 TeV the corresponding result is $(163^{+7}_{-5} \pm 9)$ pb.

At the Tevatron, the total top-pair cross section is $7.08^{+0.00+0.36}_{-0.24-0.27}$ pb [4] in very good agreement with recent results from CDF [24] and D0 [25]. Independent variation of μ_F and μ_R changes the upper scale error at the Tevatron from $+0.00$ to $+0.20$. A lot of theoretical work by many groups over the last few years (see [9] for complete references) has made possible the calculation of exact NNLO corrections. Recently, there have been numerical results of the exact NNLO contribution from the fermionic channels to the total top-pair cross section [26]. Since the $q\bar{q}$ channel is dominant at the Tevatron, this is supposed to be a good approximation to the still unknown complete NNLO at that collider. We note that our approximate NNLO results at the Tevatron are virtually indistinguishable from the results in [26] (the difference between $7.08^{+0.20}_{-0.24}$ [4] versus $7.07^{+0.20}_{-0.31}$ pb [26] for $m_t = 173$ GeV is at the per mille level with very similar scale uncertainty from independent μ_F and μ_R variation; in fact, the scale dependence of our result is slightly smaller than that of [26]), indicating that future complete NNLO results will make very little, if any, practical difference for Tevatron and probably LHC measurements of the $t\bar{t}$ cross section. We also emphasize that the comparison between exact and approximate results from resummation in [26] is quite distinct from ours since different resummation formalisms are used.

The fact that corrections beyond the soft-gluon approximation make very little difference was actually inferred from the study in [27]. The calculation there was done in both 1PI and PIM kinematics and it was shown that when terms beyond NLL are included, the difference between the results is reduced and vanishes at partonic threshold. This indicated that further terms would make very little difference, and thus, the fact that the complete NNLL terms and now the exact NNLO terms make very little difference was largely expected. This was also discussed in [28] and [4]. The more recent calculations at NNLL and NNLO prove the correctness of our earlier arguments and the robustness of our results.

No NNLO differential distributions are known at present but given the agreement of the exact and approximate NLO distributions, the agreement between the approximate and partially exact NNLO total cross sections, and the lessons learned from the comparison of approximate NLO and NNLO results calculated in 1PI and PIM kinematics, we expect that approximate NNLO should be sufficient for all practical purposes and exact NNLO results will make no significant difference to the distributions.

We also note that once the complete NNLO results are known for either the total cross section or differential distributions, the next natural step will be to add the approximate NNNLO corrections. In fact, a first study of those was performed in [29] for the $q\bar{q}$ channel at the Tevatron and it was found that the NNNLO corrections are small although not insignificant.

A major strength of our double-differential calculation is that it can be used to calculate differential distributions. Of particular significance is the study of transverse momentum and rapidity distributions. In Fig. 3, *a*, we show the top-quark transverse momentum distribution, $d\sigma/dp_T$, at the LHC. New results for 8 TeV LHC energy are plotted and compared with results at 7 TeV. The approximate NNLO top-quark p_T distributions are shown with a top-quark mass $m_t = 173$ GeV and the scale choices $\mu = m_t$ and $\mu = m_T$, where the transverse mass m_T is defined by $m_T = (p_T^2 + m_t^2)^{1/2}$. In Fig. 3, *b*, we show the K-factors, i.e., the ratios of NNLO approximate/NLO results for the top-quark p_T distribution at 8 TeV LHC energy with scale choices $\mu = m_t$ and $\mu = m_T$. We observe that the K-factor for $\mu = m_t$ rises significantly at large p_T as contrasted to that with $\mu = m_T$. The choice of the best scale is still an open question and it will be interesting to see LHC data at very high p_T. In our perturbative expansion at approximate NNLO, we have logarithms of μ_F/m_t and μ_R/m_t in plus-distribution terms as well as in $\delta(s_4)$ terms, so $\mu = m_t$ is a natural scale choice for our results.

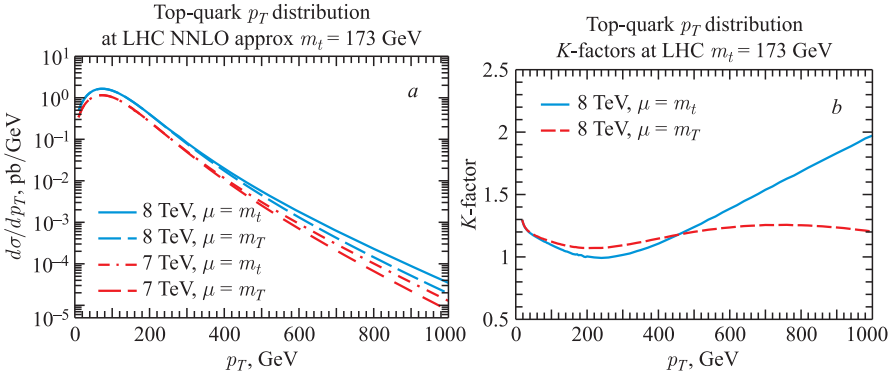

Fig. 3. NNLO approximate top-quark p_T distributions (*a*) and related K-factors (*b*) at the LHC

In Fig. 4, *a*, we present the normalized top-quark p_T distribution, $(1/\sigma)\, d\sigma/dp_T$, at 7 TeV LHC energy and compare it with recent data from CMS in the dilepton channel. We note the very good description of the CMS data by the theoretical predictions. Similar agreement is also found with CMS $l+$jets data [30] as shown in [31].

In Fig. 4, *b*, we show new results for the top-quark rapidity distribution, $d\sigma/dY$, at the LHC at 8 TeV energy and, for comparison, at 7 TeV as well. The approximate NNLO top-quark rapidity distributions are shown with a top-quark mass $m_t = 173$ GeV and the scale choice $\mu = m_t$. The NNLO soft-gluon corrections enhance the distribution without a significant change in shape relative to NLO. Our results are also in excellent agreement with CMS data [30] as shown in [31].

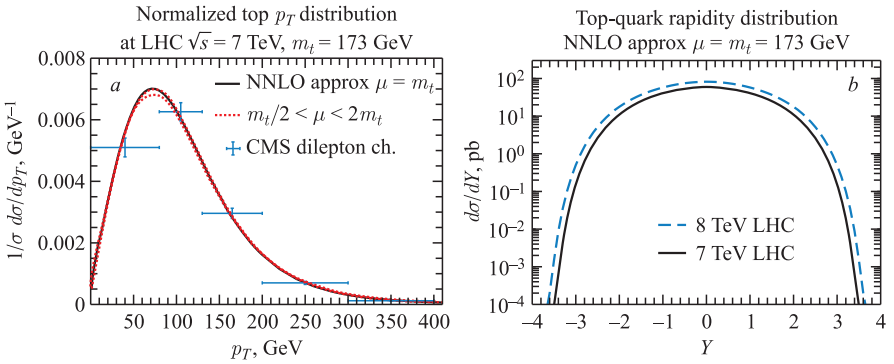

Fig. 4. NNLO approximate top-quark normalized p_T distribution compared with CMS data (*a*) and top-quark rapidity distributions (*b*) at the LHC

We also note that results for p_T distributions and for rapidity distributions and the forward–backward asymmetry at the Tevatron have been presented in [4] and [6], respectively, and a comparison with D0 data [32] shows excellent agreement [9] of our p_T distribution calculation with the Tevatron results.

3. SINGLE-TOP PRODUCTION

We continue with single-top-quark production at the LHC and the Tevatron. For the total cross sections we update results at 7 TeV [10–12] and present new results at 8 TeV LHC energy for t channel, s channel, and associated tW production. We also present new theoretical calculations and results for the single-top and single-antitop transverse momentum distributions in t-channel production at the Tevatron and at 7 and 8 TeV energy at the LHC and in tW production at the LHC. As for top-pair production, we note that the agreement between exact

NLO [33, 34] and approximate NLO cross sections for all three single-top channels is very good, which again serves as the motivation to derive approximate NNLO results.

At the leading order, the partonic processes for t-channel production are $qb \to q't$ and $\bar{q}b \to \bar{q}'t$; for s-channel production, $q\bar{q}' \to \bar{b}t$; and for associated tW production, $bg \to tW^-$. At the Tevatron the cross sections for single-top production in all three channels are identical to those for single antitop. However, at the LHC the t-channel and s-channel single-top cross sections are larger than those for antitop.

In Tables 1 and 2, we present for 7 and 8 TeV LHC energy, respectively, the total NNLO approximate cross sections, derived from NNLL resummation, for single-top production in the t channel, s channel, and in tW production. Separate results are given for single top, single antitop, and the combined sum. In each case, the central result is for $\mu = m_t$, the first uncertainty is from scale variation $m_t/2 < \mu < 2m_t$, and the second uncertainty is from the MSTW2008 NNLO pdf sets at 90% C.L. [20]. The t channel has the largest cross section, followed by tW production, with the s channel numerically the smallest. Our theoretical results for the Tevatron can be found in [10, 12] and they are in good agreement with the recent Tevatron data; the total cross section that we find for the sum of t plus s channels is $3.16^{+0.18}_{-0.19}$ pb for $m_t = 172.5$ GeV which agrees well with the results of $3.04^{+0.57}_{-0.53}$ pb from CDF [35] and $3.43^{+0.73}_{-0.74}$ pb from D0 [36].

Table 1. **Results for single-top, single-antitop, and combined approximate NNLO cross sections at 7 TeV LHC energy with $m_t = 173$ GeV in pb**

LHC 7 TeV	$\sigma(t)$, pb	$\sigma(\bar{t})$, pb	$\sigma(t) + \sigma(\bar{t})$, pb
t channel	$43.0^{+1.6}_{-0.2} \pm 0.8$	$22.9 \pm 0.5^{+0.7}_{-0.9}$	$65.9^{+2.1\,+1.5}_{-0.7\,-1.7}$
s channel	$3.14 \pm 0.06^{+0.12}_{-0.10}$	$1.42 \pm 0.01^{+0.06}_{-0.07}$	$4.56 \pm 0.07^{+0.18}_{-0.17}$
tW	$7.8 \pm 0.2^{+0.5}_{-0.6}$	$7.8 \pm 0.2^{+0.5}_{-0.6}$	$15.6 \pm 0.4 \pm 1.1$

Table 2. **Results for single-top, single-antitop, and combined approximate NNLO cross sections at 8 TeV LHC energy with $m_t = 173$ GeV in pb**

LHC 8 TeV	$\sigma(t)$, pb	$\sigma(\bar{t})$, pb	$\sigma(t) + \sigma(\bar{t})$, pb
t channel	$56.4^{+2.1}_{-0.3} \pm 1.1$	$30.7 \pm 0.7^{+0.9}_{-1.1}$	$87.2^{+2.8\,+2.0}_{-1.0\,-2.2}$
s channel	$3.79 \pm 0.07 \pm 0.13$	$1.76 \pm 0.01 \pm 0.08$	$5.55 \pm 0.08 \pm 0.21$
tW	$11.1 \pm 0.3 \pm 0.7$	$11.1 \pm 0.3 \pm 0.7$	$22.2 \pm 0.6 \pm 1.4$

In Fig. 5, *a*, we show the total cross sections for the three single-top channels versus the LHC energy, with the central result for $\mu = m_t$, and the scale and pdf uncertainties added in quadrature. The t-channel results are in very good agreement with LHC data from both ATLAS and CMS at 7 TeV [37, 38] and 8 TeV [39, 40]. The tW results at 7 TeV are also in excellent agreement with

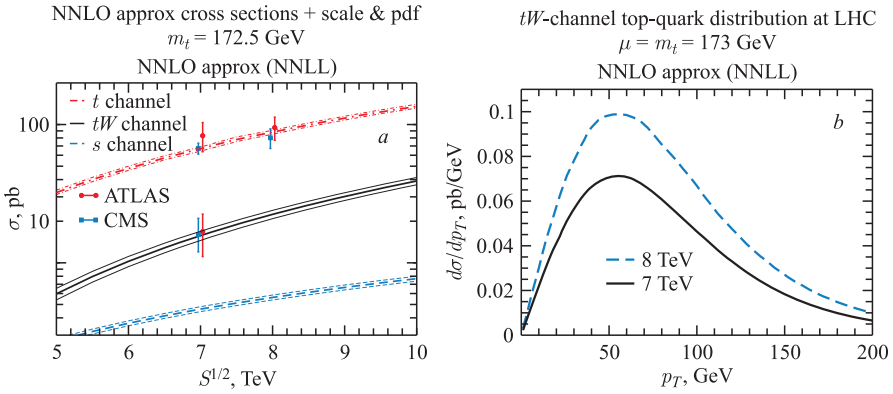

Fig. 5. *a*) Total $\sigma(t) + \sigma(\bar{t})$ approximate NNLO cross sections in all three single-top channels compared with data from the LHC; *b*) tW-channel top-quark p_T distribution at the LHC

the data from ATLAS [41] and CMS [42]. At present, there is only a limit on the s-channel cross section < 26 pb at 95% C.L. [43].

We also note that the ratio of the single-top and single-antitop cross sections in the t channel has been measured by ATLAS [44] at 7 TeV LHC energy. The ATLAS result of $1.81^{+0.23}_{-0.22}$ is in excellent agreement with our calculation of $1.88^{+0.11}_{-0.09}$.

In Fig. 5, *b*, we show results from a new calculation for the top-quark transverse momentum distribution in tW production at the LHC at both 7 and 8 TeV collider energy.

In Fig. 6, we show new results for the top-quark transverse momentum distribution in t-channel single-top production at the LHC and the Tevatron (plot *a*)

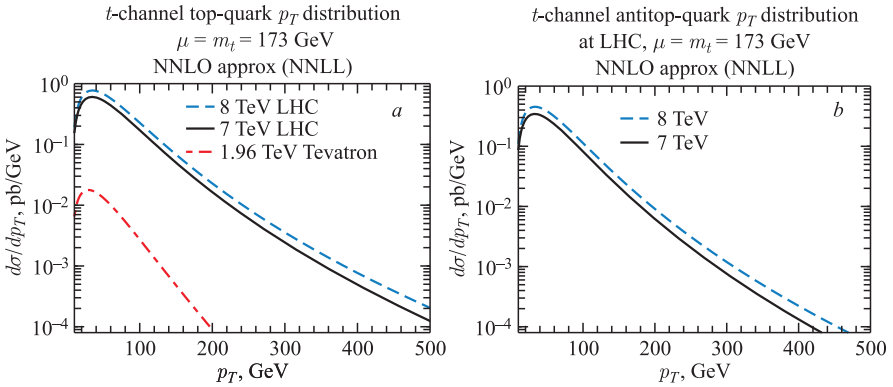

Fig. 6. t-channel approximate NNLO top-quark (*a*) and antitop-quark (*b*) p_T distributions at the LHC and the Tevatron

and the antitop-quark transverse momentum distribution in t-channel production at the LHC (plot b).

CONCLUSION

The threshold resummation of soft-gluon contributions provides a powerful method to accurately calculate top-quark total cross sections and differential distributions for both top-pair and single-top production. Resummation is performed at NNLL accuracy for the double-differential cross section and used to provide approximate NNLO results for total and differential cross sections. We have shown the applicability, validity, and accuracy of the approach by explicit comparisons to complete NLO and partial NNLO calculations. The comparisons show that currently available partial exact NNLO corrections are virtually indistinguishable from the NNLO approximations in our formalism (which is distinct from other resummation formalisms) both in the central result and in the theoretical uncertainty, and they thus indicate that future complete NNLO corrections will very likely have a negligible impact on the existing results from our formalism. New state-of-the-art results for top-pair and single-top total cross sections and transverse momentum and rapidity distributions are presented at the LHC and Tevatron energies, with particular attention to the 8 TeV LHC energy. All theoretical results, for both $t\bar{t}$ and single-top production, and for both total cross sections and differential distributions, are in excellent agreement with the recent LHC and Tevatron data.

Acknowledgements. This material is based upon work supported by the National Science Foundation under Grant No. PHY 1212472.

REFERENCES

1. *Kidonakis N., Sterman G.* Subleading Logarithms in QCD Hard Scattering // Phys. Lett. B. 1996. V. 387. P. 867–874.
2. *Kidonakis N., Sterman G.* Resummation for QCD Hard Scattering // Nucl. Phys. B. 1997. V. 505. P. 321–348; arXiv:hep-ph/9705234.
3. *Ahrens V. et al.* Renormalization-Group Improved Predictions for Top-Quark Pair Production at Hadron Colliders // JHEP. 2010. V. 1009. P. 097; arXiv:1003.5827[hep-ph].
4. *Kidonakis N.* Next-to-Next-to-Leading Soft-Gluon Corrections for the Top-Quark Cross Section and Transverse Momentum Distribution // Phys. Rev. D. 2010. V. 82. P. 114030; arXiv:1009.4935[hep-ph].
5. *Ahrens V. et al.* RG-Improved Single-Particle Inclusive Cross Sections and Forward-Backward Asymmetry in $t\bar{t}$ Production at Hadron Colliders // JHEP. 2011. V. 1109. P. 070; arXiv:1103.0550[hep-ph].

6. *Kidonakis N.* Top-Quark Rapidity Distribution and Forward-Backward Asymmetry // Phys. Rev. D. 2011. V. 84. P. 011504; arXiv:1105.5167[hep-ph].
7. *Aliev M. et al.* HATHOR: Hadronic Top and Heavy Quarks Cross Section Calculator // Comp. Phys. Commun. 2011. V. 182. P. 1034–1046; arXiv:1007.1327[hep-ph].
8. *Beneke M. et al.* Hadronic Top-Quark Pair Production with NNLL Threshold Resummation // Nucl. Phys. B. 2012. V. 855. P. 695–741; arXiv:1109.1536[hep-ph].
9. *Kidonakis N., Pecjak B. D.* Top-Quark Production and QCD // Eur. Phys. J. C. 2012. V. 72. P. 2084; arXiv:1108.6063[hep-ph].
10. *Kidonakis N.* Next-to-Next-to-Leading Logarithm Resummation for s-Channel Single-Top-Quark Production // Phys. Rev. D. 2010. V. 81. P. 054028; arXiv:1001.5034[hep-ph].
11. *Kidonakis N.* Two-Loop Soft Anomalous Dimensions for Single-Top-Quark Associated Production with a W^- or H^- // Phys. Rev. D. 2010. V. 82. P. 054018; arXiv:1005.4451[hep-ph].
12. *Kidonakis N.* Next-to-Next-to-Leading-Order Collinear and Soft Gluon Corrections for t-Channel Single-Top-Quark Production // Phys. Rev. D. 2011. V. 83. P. 091503; arXiv:1103.2792[hep-ph].
13. *Sterman G.* Summation of Large Corrections to Short Distance Hadronic Cross Sections // Nucl. Phys. B. 1987. V. 281. P. 310–364.
14. *Catani S., Trentadue L.* Resummation of the QCD Perturbative Series for Hard Processes // Nucl. Phys. B. 1989. V. 327. P. 323–352.
15. *Kidonakis N.* Second-Order Approximate Corrections for QCD Processes // DPF 2011. eConf C110809; arXiv:1109.1578[hep-ph].
16. *Kidonakis N.* Two-Loop Soft Anomalous Dimensions and Next-to-Next-to-Leading-Logarithm Resummation for Heavy Quark Production // Phys. Rev. Lett. 2009. V. 102. P. 232003; arXiv:0903.2561[hep-ph].
17. *Nason P., Dawson S., Ellis R. K.* The Total Cross Section for the Production of Heavy Quarks in Hadronic Collisions // Nucl. Phys. B. 1988. V. 303. P. 607–633.
18. *Beenakker W. et al.* QCD Corrections to Heavy-Quark Production in $p\bar{p}$ Collisions // Phys. Rev. D. 1989. V. 40. P. 54–82.
19. *Beenakker W. et al.* QCD Corrections to Heavy Quark Production in Hadron–Hadron Collisions // Nucl. Phys. B. 1991. V. 351. P. 507–560.
20. *Martin A. D. et al.* Parton Distributions for the LHC // Eur. Phys. J. C. 2009. V. 63. P. 189–285; arXiv:0901.0002[hep-ph].
21. *ATLAS Collab.* Measurement of the Top-Quark Pair Production Cross Section with ATLAS in pp Collisions at $\sqrt{s} = 7$ TeV in the Single-Lepton Channel Using Semileptonic b Decays. ATLAS-CONF-2012-131.
22. *CMS Collab.* Combination of Top-Quark Pair Production Cross-Section Measurements. CMS-PAS-TOP-11-024.

23. *CMS Collab.* Measurement of the $t\bar{t}$ Production Cross Section in the Dilepton Channel in pp Collisions at $\sqrt{s} = 8$ TeV. CMS-PAS-TOP-12-007.
24. *CDF Collab.* Top Dilepton Cross Section in 5.1 fb^{-1} Using the DIL Selection. Conf. Note 10163.
25. *D0 Collab.* Measurement of the $t\bar{t}$ Production Cross Section Using Dilepton Events in $p\bar{p}$ Collisions // Phys. Lett. B. 2011. V. 704. P. 403–410; arXiv:1105.5384[hep-ex].
26. *Baernreuther P., Czakon M., Mitov A.* Percent-Level-Precision Physics at the Tevatron: Next-to-Next-to-Leading Order QCD Corrections to $q\bar{q} \to t\bar{t} + X$ // Phys. Rev. Lett. 2012. V. 109. P. 132001; arXiv:1204.5201[hep-ph].
27. *Kidonakis N., Vogt R.* Next-to-Next-to-Leading Order Soft-Gluon Corrections in Top-Quark Hadroproduction // Phys. Rev. D. 2003. V. 68. P. 114014; arXiv:hep-ph/0308222.
28. *Kidonakis N., Vogt R.* Theoretical Top-Quark Cross Section at the Fermilab Tevatron and the CERN LHC // Phys. Rev. D. 2008. V. 78. P. 074005; arXiv:0805.3844[hep-ph].
29. *Kidonakis N.* Next-to-Next-to-Next-to-Leading-Order Soft-Gluon Corrections in Hard-Scattering Processes near Threshold // Phys. Rev. D. 2006. V. 73. P. 034001; arXiv:hep-ph/0509079.
30. *CMS Collab.* Measurement of Differential Top-Quark Pair Production Cross Sections in pp Collisions at $\sqrt{s} = 7$ TeV. arXiv:1211.2220[hep-ex].
31. *Kidonakis N.* Single-Top and Top-Pair Production. arXiv:1212.2844[hep-ph].
32. *D0 Collab.* Dependence of the $t\bar{t}$-Production Cross Section on the Transverse Momentum of the Top Quark // Phys. Lett. B. 2010. V. 693. P. 515–521; arXiv:1001.1900[hep-ex].
33. *Harris B. W. et al.* Fully Differential Single-Top-Quark Cross Section in Next-to-Leading Order QCD // Phys. Rev. D. 2002. V. 66. P. 054024; arXiv:hep-ph/0207055.
34. *Zhu S.* Next-to-Leading Order QCD Corrections to $bg \to tW^-$ at the CERN Large Hadron Collider // Phys. Lett. B. 2002. V. 524. P. 283–288; Erratum // Ibid. V. 537. P. 351–352.
35. *CDF Collab.* Measurement of Single-Top-Quark Production in 7.5 fb^{-1} of CDF Data Using Neural Networks. CDF Note 10793.
36. *D0 Collab.* Measurements of Single-Top-Quark Production Cross Sections and $|V_{tb}|$ in $p\bar{p}$ Collisions at $\sqrt{s} = 1.96$ TeV // Phys. Rev. D. 2011. V. 84. P. 112001; arXiv:1108.3091[hep-ex].
37. *ATLAS Collab.* Measurement of the t-Channel Single-Top-Quark Production Cross Section in pp Collisions at $\sqrt{s} = 7$ TeV with the ATLAS Detector. arXiv:1205.3130[hep-ex].
38. *CMS Collab.* Measurement of the Single-Top-Quark t-Channel Cross Section in pp Collisions at $\sqrt{s} = 7$ TeV. arXiv:1209.4533[hep-ex].
39. *ATLAS Collab.* Measurement of t-Channel Single-Top-Quark Production in pp Collisions at $\sqrt{s} = 8$ TeV with the ATLAS Detector. ATLAS-CONF-2012-132.

40. *CMS Collab.* Measurement of the Single-Top-Quark t-Channel Cross Section in pp Collisions at $\sqrt{s} = 8$ TeV. CMS-PAS-TOP-12-011.

41. *ATLAS Collab.* Evidence for the Associated Production of a W Boson and a Top Quark in ATLAS at $\sqrt{s} = 7$ TeV // Phys. Lett. B. 2012. V. 716. P. 142–159; arXiv:1205.5764[hep-ex].

42. *CMS Collab.* Evidence for Associated Production of a Single-Top-Quark and W Boson in pp Collisions at 7 TeV. arXiv:1209.3489[hep-ex].

43. *ATLAS Collab.* Search for s-Channel Single-Top-Quark Production in pp Collisions at $\sqrt{s} = 7$ TeV. ATLAS-CONF-2011-118.

44. *ATLAS Collab.* Measurement of the t-Channel Single-Top-Quark and Top-Antiquark Cross Sections and Their Ratio in pp Collisions at $\sqrt{s} = 7$ TeV. ATLAS-CONF-2012-056.